

XeF₂ gas-assisted focused-electron-beam-induced etching of GaAs with 30 nm resolution

A Ganczarczyk, M Geller and A Lorke

Faculty of Physics and CeNIDE, University of Duisburg-Essen, Lotharstraße 1, 47048 Duisburg, Germany

E-mail: arkadius.ganczarczyk@uni-due.de

Received 20 September 2010, in final form 15 November 2010

Published 15 December 2010

Online at stacks.iop.org/Nano/22/045301

Abstract

We demonstrate the gas-assisted focused-electron-beam (FEB)-induced etching of GaAs with a resolution of 30 nm at room temperature. We use a scanning electron microscope (SEM) in a dual beam focused ion beam together with xenon difluoride (XeF₂) that can be injected by a needle directly onto the sample surface. We show that the FEB-induced etching with XeF₂ as a precursor gas results in isotropic and smooth etching of GaAs, while the etch rate depends strongly on the beam current and the electron energy. The natural oxide of GaAs at the sample surface inhibits the etching process; hence, oxide removal in combination with chemical surface passivation is necessary as a strategy to enable this high-resolution etching alternative for GaAs.

1. Introduction

The possibility to manipulate and process material at the nanometer scale is the origin for the ongoing success of nano-science and -technology. Direct, i.e. not resist-based, patterning techniques are an interesting alternative to the most common patterning technique on the nanometer scale: electron beam lithography (EBL). In particular the focused ion beam (FIB) method has been proven to be a very easy and fast method for material processing on the nanoscale [1, 2]. Although a resolution comparable to that of EBL can be achieved [3, 4], the structural damage and the ion implantation induced by energetic ion bombardment is a main drawback of FIB patterning [5–8], especially for electrically active materials [9, 10]. A possibility to reduce FIB-induced damage is the use of low energy ions, but at the cost of resolution inherent to a low energy focused ion beam [11]. And although the usage of gas-assisted FIB patterning is less invasive than pure FIB milling, the damage caused by the ion beam is still substantial [5, 6].

A less destructive technique is the gas-assisted etching induced by a focused-electron-beam (FEB). The FEB patterning of a variety of materials has been reported so far [12, 13], e.g. for PMMA [14], Si [14–19] or SiO₂ [16, 20] with molecular chlorine (Cl₂) or xenon difluoride (XeF₂)

as the precursor gases. The FEB-induced etching of GaAs was achieved using molecular chlorine as the etching agent [14, 21–24]. However, various drawbacks, such as a very low etch rate and resolution, the requirement of a heated substrate or *in situ* wafer growth have limited the use of the FEB-induced etching of GaAs with Cl₂.

Here, we report on the room temperature gas-assisted FEB-induced etching of GaAs with nanometer resolution. We use a scanning electron microscope (SEM) in a FEI Helios Nanolab 600 dualbeam FIB/SEM system together with a xenon difluoride (XeF₂) precursor gas injection system. The etching agent can be injected by a needle directly onto the sample surface. It is shown that for a successful FEB-induced etching process, the native surface oxide layer of GaAs has to be removed with subsequent chemical passivation of the surface. We demonstrate a writing resolution down to 30 nm with a surface roughness considerably smaller than the structure size. Furthermore, we investigate the dependence of the etching resolution and the etching rate on various parameters, such as the beam current and electron acceleration voltage.

2. Experimental details

First experiments with FEB-induced etching showed that the thin native surface oxide layer [25, 26] prevents the successful

etching of GaAs. Therefore, the following recipe is used prior to FEB etching to remove and passivate the GaAs substrate. After a thorough cleaning of the GaAs substrate, the sample is etched for 15 s in 3:1:100 piranha acid ($\text{H}_2\text{SO}_4\text{:H}_2\text{O}_2\text{:H}_2\text{O}$). After the etching step the sample is immediately transferred into a 20% aqueous solution of $(\text{NH}_4)_2\text{S}$ for 1 min. The sample is rinsed two times for 3 s with deionized water to remove the excess $(\text{NH}_4)_2\text{S}$, blown dry with N_2 and transferred into the FIB chamber.

The resulting chemical passivation of the GaAs surface with sulfur is used here to prevent the re-oxidization of the GaAs surface, since GaAs oxidates immediately when brought into contact with air [25]. The sulfur establishes a volatile compound with the As-atoms on the GaAs surface, which can be easily cracked by FEB-induced etching. The chemical surface passivation of GaAs can be accomplished with solutions of inorganic sulfides such as sodium sulfide (Na_2S) or ammonium sulfide ($(\text{NH}_4)_2\text{S}$) [27–30].

3. Results and discussion

Figure 1(a) shows a SEM image of a GaAs surface after passivation as described above and FEB-induced etching with XeF_2 . Four trenches were etched with an electron acceleration voltage of $V = 10$ kV, a beam current of $I = 1.4$ nA and etching times of (from left to right) $t = 16, 12, 8$ and 4 min. The dwell time is kept at the minimum value of 100 ns in order to maximize the etch rate [20]. The nominal scanned area of all trenches is $500 \text{ nm} \times 30 \text{ nm}$, however, the resulting etched area increases with increasing etching time. For an etching time of $t = 4$ min, an etched trench is barely visible, while the width of the other three trenches increases from 38 up to 48 nm.

The actual depth and shape of the trenches and their surface roughness can be seen in figure 1(b). The figure shows a SEM image of the cross-section of the etched trenches shown in figure 1(a). Using standard FIB milling, the substrate was partially removed (up to the white line indicated in figure 1(a)) and the sample was imaged under 45° as illustrated in the inset. The trench on the right with the lowest etching time of $t = 4$ min is barely visible, indicating that the FEB-induced etching has not penetrated the surface and only a minor morphology change of the surface took place. The trench with an etching time of $t = 16$ min has a width of 48 nm at the surface and a depth of 180 nm. The trenches with an etching time of $t = 12$ and 8 min have a width of 44 nm and 38 nm at the surface and a depth of 130 nm and 100 nm, respectively. Note the sharp borders of the trenches, nicely visible in the cross-section view in figure 1(b).

The broadening of the trenches seems to be caused by lateral etching, which can be explained by two mechanisms: firstly, secondary and backscattered electrons can dissociate surface adsorbed molecules in the non-scanned area of the surface. Secondly, after the dissociation of the precursor gas molecules the mobility of the reactive species can cause etching parallel to the sample surface, leading to a cone-shaped cross-section etch profile (see figure 1(b)), well known from wet-chemical etch processes. In addition, a sample drift might be present for long etching times (see the trenches for $t =$

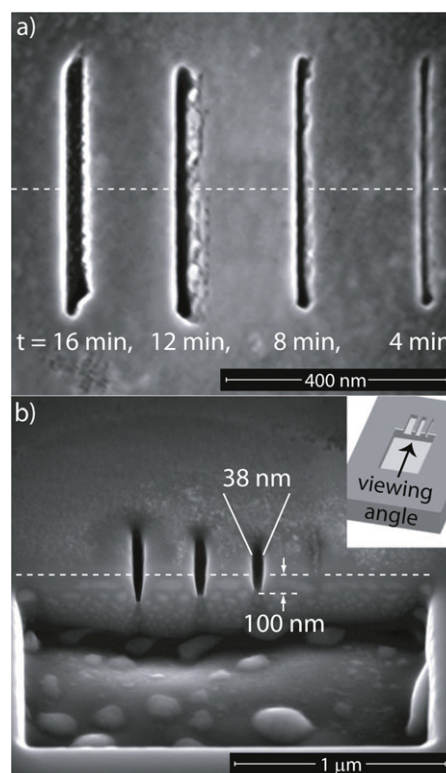


Figure 1. (a) SEM image of a $(\text{NH}_4)_2\text{S}$ passivated GaAs surface after exposure to FEB etching with XeF_2 as the precursor gas. Four trenches were etched with an electron acceleration voltage of $V = 10$ kV, a beam current of $I = 1.4$ nA and etching times (from left to right) of $t = 16, 12, 8$ and 4 min. The nominal scanned area of all trenches is $500 \text{ nm} \times 30 \text{ nm}$. (b) SEM image of the cross-section of the etched trenches shown in (a). The sample was tilted by 45° and the substrate below the white line was removed with a focused ion beam (FIB) to a depth of 500 nm, illustrated in the inset.

12 and 16 min in figure 1(a)), since the bottom/top edge of the trenches exhibit no rectangular corners. The low surface roughness of the trenches can be explained through the non-selective etching of GaAs by XeF_2 .¹ Due to the relatively long etch times a light sample drift can be observed in figure 1(a), see especially the trenches for $t = 12$ and 16 min.

Figure 2 shows the maximum resolution achieved so far using this FEB etching technique. The electron acceleration voltage was set to $V = 20$ kV and a beam current and etching time of $I = 1.4$ nA and $t = 5$ min, respectively, were used. The nominal scanned area of this trench is $500 \text{ nm} \times 20 \text{ nm}$. The resulting width of the etched trench is ≈ 30 nm with a surface roughness which is considerably smaller than the structure size.

Figure 3 shows the etched trench volume W as a function of the etching time t for beam currents of $I = 1.4$ nA (red points), $I = 5.6$ nA (blue points) and $I = 11$ nA (green points). The acceleration voltage is fixed to $V = 10$ kV, while

¹ The physical mechanisms underlying the FEB-induced etching technique will not be covered here in detail. For further reading, see the review papers of Utke *et al* [13] and Randolph *et al* [12] and the references cited therein. Furthermore, the interaction of adsorbed XeF_2 -molecules with GaAs with and without electron beam support has been described in detail by Varekamp *et al* and Nienhaus and Moench [31, 32].

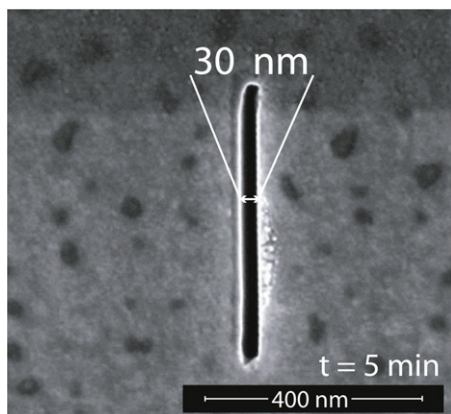


Figure 2. SEM image of a $(\text{NH}_4)_2\text{S}$ passivated GaAs surface after exposure to FEB etching with a XeF_2 precursor gas. One trench was etched with an electron acceleration voltage of $V = 20$ kV, a beam current of $I = 1.4$ nA and an etching time of $t = 5$ min.

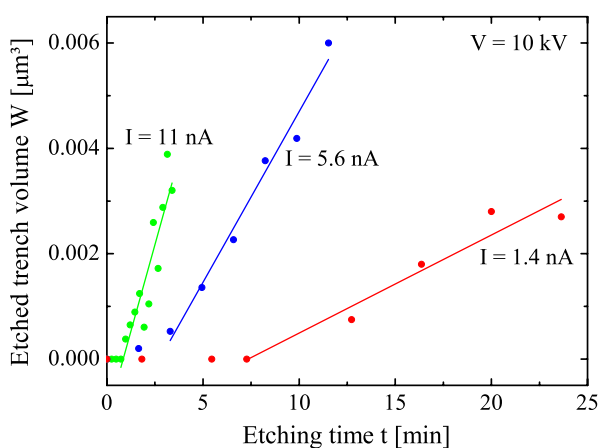


Figure 3. Dependence of the etched trench volume W on the etching time t for beam currents $I = 1.4$ nA (red dots), $I = 5.6$ nA (blue dots) and $I = 11$ nA (yellow dots) and an electron acceleration voltage of $V = 10$ kV. The corresponding lines are fits to the linear part of the data yielding etching rates of $0.2 \times 10^{-3} \mu\text{m}^3 \text{min}^{-1}$, $0.65 \times 10^{-3} \mu\text{m}^3 \text{min}^{-1}$ and $1.3 \times 10^{-3} \mu\text{m}^3 \text{min}^{-1}$, respectively. (This figure is in colour only in the electronic version)

the dwell time is again kept at 100 ns. For the evaluation of the etched volume, the trenches were approximated by a cuboid shape. For all beam currents, the etched volume W remains almost zero for a time increasing from approximately 1 min (for the highest beam current of $I = 11$ nA) up to 7 min (for the lowest beam current of $I = 1.4$ nA). Afterward, a linear increase of the etched volume W with the etching time t sets in. From a linear fit (colored lines in figure 3) we obtain an etch rate of $0.2 \times 10^{-3} \mu\text{m}^3 \text{min}^{-1}$, $0.65 \times 10^{-3} \mu\text{m}^3 \text{min}^{-1}$ and $1.3 \times 10^{-3} \mu\text{m}^3 \text{min}^{-1}$ for beam currents $I = 1.4$ nA (red points), $I = 5.6$ nA (blue points) and $I = 11$ nA, respectively.

The delayed etching observed in the curves of figure 3 suggests that the chemical treatment using the method described above does not lead to a completely passivated

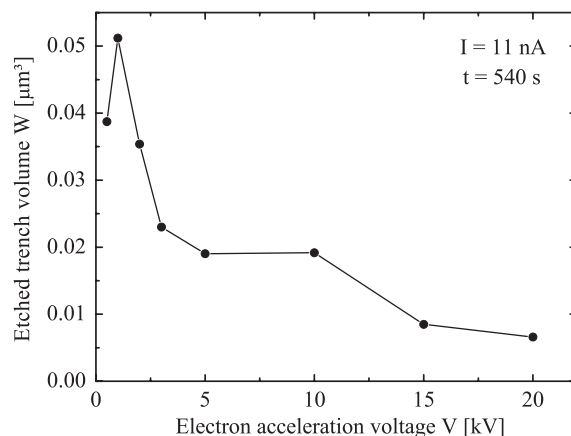


Figure 4. Dependence of the etched trench volume W on the electron acceleration voltage V with a beam current of $I = 11$ nA and an etching time of $t = 540$ s.

surface of the GaAs substrate. Therefore, the FEB-induced etching cannot immediately penetrate the surface, a conclusion that is supported by the cross-sectional image of the etched trench in figure 1(a) for a short etching time of 4 min. It is likely that a thin oxide layer has remained or is reformed on the surface, as the sulfur compounds on the sample are volatile [28] and re-oxidation occurs quickly [25]. Additionally the surface passivation in an aqueous solution of $(\text{NH}_4)_2\text{S}$ can cause a reformation of a very thin GaAs oxide layer [33]. Using sodium sulfide instead of ammonium sulfide and isopropanol or butanol as a solvent rather than water [33] could therefore improve the passivation of the GaAs surface. Another explanation for the delayed onset of etching might be carbon surface contamination that can potentially inhibit the etch process [12].

The volume etch rates depend approximately linearly on the beam current I and we cannot find any saturation current up to 22 nA. In addition, we find a strong dependence of the volume etch rate on the electron acceleration voltage V , shown in figure 4. In this figure, the trench volume W after the 540 s FEB etch at $I = 11$ nA is plotted as a function of the acceleration voltage V . The volume etch rate increases between $V = 300$ V and 1 kV. For $V > 1$ kV the volume etch rate decreases again with an approximately inverse dependence on the acceleration voltage V . The maximum volume etch rate is located in the low energy region between $V = 300$ V and 2 kV. A similar behavior for $V > 1$ kV was observed in references [19, 20] and can be explained by the dissociation cross-section of electrons with adsorbed or gas phase XeF_2 molecules that decreases for higher electron energies. For lower electron energies ($V < 1$ kV), a maximum in the dissociation cross-section is generally observed in the incident electron range of $V = 100$ V–1 kV for different precursor gases [12, 13, 34–36], e.g. for Cl_2 , $\text{W}(\text{CO})_6$ and WF_6 .² A further effect has to be mentioned concerning the FEB etching dependence on the acceleration voltage V . As mentioned in the

² Data for XeF_2 is not available, as irradiation data for etching agents used in FEB-induced etching is very rare.

description of figure 2, the best resolution was achieved at $V = 20$ kV, however, with a low etch rate (see figure 4). In general, the achieved resolution is increased by increasing the electron energy. However, the etching rate decreases simultaneously causing longer etching times. To obtain reasonable etching times, this either limits the size of high-resolution structures or limits the resolution of larger structures. In addition, sample drift may practically limit the high-resolution patterning for long etching times (see figure 1(a)).

4. Conclusion

In summary, we demonstrate the room temperature gas-assisted FEB etching of GaAs with nanometer scale resolution. A resolution of 30 nm with a surface roughness considerably smaller than the structure size is achieved. Prior the etching step, the natural oxide surface layer of GaAs has to be removed with subsequent chemical passivation of the GaAs surface with $(\text{NH}_4)_2\text{S}$. The volume etch rate depends linearly on the electron beam current. With increasing electron energy the resolution and surface roughness improves, however, the etch rate decreases simultaneously.

Acknowledgments

We thank Hermann Nienhaus and Cedrik Meier for very fruitful discussions. The authors gratefully acknowledge financial support under Grant No. 03X0112B by the BMBF and by the DFG in the framework of the NanoSci-E + project QD2D of the European Commission.

References

- [1] Li H W, Kang D J, Blamire M G and Huck W T S 2003 Focused ion beam fabrication of silicon print masters *Nanotechnology* **14** 220–3
- [2] Tseng A A 2005 Recent developments in nanofabrication using focused ion beams *Small* **1** 924–39
- [3] Gazzadi G C, Angeli E, Facci P and Frabboni S 2006 Electrical characterization and Auger depth profiling of nanogap electrodes fabricated by I_2 -assisted focused ion beam *Appl. Phys. Lett.* **89** 173112
- [4] Nagase T, Gamo K, Kubota T and Mashiko S 2006 Direct fabrication of nano-gap electrodes by focused ion beam etching *Thin Solid Films* **499** 279
- [5] Sugimoto Y, Taneya M, Hidaka H and Akita K 1990 Reduction of induced damage in GaAs processed by Ga^+ focused-ion-beam-assisted Cl_2 etching *J. Appl. Phys.* **68** 2392–9
- [6] Akita K, Taneya M, Sugimoto Y, Hidaka H and Tajima M 1990 Evaluation of the stopping depth of nonradiative recombination centers in $\text{Al}_{0.5}\text{Ga}_{0.5}\text{As}$ by Ar^+ ion beam sputtering by photoluminescence measurements *J. Vac. Sci. Technol. A* **8** 3274–8
- [7] Ishitani T and Yaguchi T 1996 Cross-sectional sample preparation by focused ion beam: a review of ion-sample interaction *Microsc. Res. Technol.* **35** 320–33
- [8] Langford R M and Petford-Long A K 2001 Preparation of transmission electron microscopy cross-section specimens using focused ion beam milling *J. Vac. Sci. Technol. A* **19** 2186–93
- [9] Hirayama Y, Saku T and Horikoshi Y 1989 Electronic transport through very short and narrow channels constricted in GaAs by highly resistive Ga-implanted regions *Phys. Rev. B* **39** 5535–7
- [10] Wieck A D and Ploog K 1989 In-plane-gated quantum wire transistor fabricated with directly written focused ion beams *Appl. Phys. Lett.* **56** 928–30
- [11] Liang T, Stivers A, Livengood R, Yan P Y, Zhang G and Lo F C 2000 Progress in extreme ultraviolet mask repair using a focused ion beam *J. Vac. Sci. Technol. B* **18** 3216–20
- [12] Randolph S J, Fowlkes J D and Rack P D 2006 Focused, nanoscale electron-beam-induced deposition and etching *Crit. Rev. Solid State Mater. Sci.* **31** 55–89
- [13] Utke I, Hoffmann P and Melngailis J 2008 Gas-assisted focused electron beam and ion beam processing and fabrication *J. Vac. Sci. Technol. B* **26** 1197–276
- [14] Matsui S, Ichihashi T and Mito M 1989 Electron beam induced selective etching and deposition technology *J. Vac. Sci. Technol. B* **6** 1182–90
- [15] Winters H F and Coburn J W 1978 The etching of silicon with XeF_2 vapor *Appl. Phys. Lett.* **34** 70
- [16] Coburn J W and Winters H F 1979 Ion-and electron-assisted gas-surface chemistry—an important effect in plasma etching *J. Appl. Phys.* **50** 3189–96
- [17] Matsui S and Katsumi H 1987 Direct writing onto Si by electron beam stimulated etching *Appl. Phys. Lett.* **51** 1498–9
- [18] Yemini M, Hadad B, Liebes Y, Goldner A and Ashkenasy N 2009 The controlled fabrication of nanopores by focused electron-beam-induced etching *Nanotechnology* **20** 245302
- [19] Roediger P, Hochleitner G, Bertagnolli E, Wanzenboeck H D and Buehler W 2010 Focused electron beam induced etching of silicon using chlorine *Nanotechnology* **21** 285306
- [20] Randolph S J, Fowlkes J D and Rack P D 2005 Focused electron-beam-induced etching of silicon dioxide *J. Appl. Phys.* **98** 034902
- [21] Taneya M, Sugimoto Y, Hidaka H and Akita K 1989 Electron-beam-induced Cl_2 etching of GaAs *Japan. J. Appl. Phys.* **28** 515–7
- [22] Akita K, Sugimoto Y and Kawanishi H 1991 Electron-beam-induced maskless HCl pattern etching of GaAs *Semicond. Sci. Technol.* **6** 934–6
- [23] Sugimoto Y, Taneya M, Akita K and Kawanishi H 1991 Novel *in situ* pattern etching of GaAs by electron-beam-stimulated oxidation and subsequent Cl_2 gas etching *J. Appl. Phys.* **69** 2725–7
- [24] Kohmoto S, Sugimoto Y, Takado N and Asakawa K 1994 *In situ* GaAs/AlGaAs patterning using a thin epitaxial InGaAs layer mask as a negative-type electron-beam resist in Cl_2 gas *J. Vac. Sci. Technol. B* **12** 3699–703
- [25] Lukes F 1972 Oxidation of Si and GaAs in air at room temperature *Surf. Sci.* **30** 91–100
- [26] Chang C C, Citrin P H and Schwartz B 1977 Chemical preparation of GaAs surfaces and their characterization by Auger electron and x-ray photoemission spectroscopies *J. Vac. Sci. Technol.* **14** 943–52
- [27] Sandroff C J, Nottenburg R N, Bischoff J C and Bhat R 1987 Dramatic enhancement in the gain of a GaAs/AlGaAs heterostructure bipolar transistor by surface chemical passivation *Appl. Phys. Lett.* **51** 33–5

- [28] Lee H H, Racicot R J and Lee S H 1988 Surface passivation of GaAs *Appl. Phys. Lett.* **54** 724–6
- [29] Yablonovitch E, Gmitter T and Bagley B G 1990 As₂S₃/GaAs, a new amorphous/crystalline heterojunction for the III–V semiconductors *Appl. Phys. Lett.* **57** 2241–3
- [30] Bessolov V N, Konenkova E V and Lebedev M V 1996 Solvent effect on the properties of sulfur passivated GaAs *J. Vac. Sci. Technol. B* **14** 2761–6
- [31] Varekamp P R, Simpson W C, Shuh D K, Durbin T D, Chakarian V and Yarmoff J A 1994 Electronic structure of GaF₃ films grown on GaAs via exposure to XeF₂ *Phys. Rev. B* **50** 14267–76
- [32] Nienhaus H and Moench W 1996 Fluorine adsorption on GaAs (110) surfaces and the onset of etching after XeF₂ exposures *Appl. Surf. Sci.* **104** 95–100
- [33] Bessolov V N, Konenkova E V and Lebedev M V 1997 A comparison of the effectiveness of GaAs surface passivation with sodium and ammonium sulfide solutions *Phys. Solid State* **39** 54–7
- [34] Hoyle P C, Cleaver J R A and Ahmed H 1994 Ultralow energy focused electron beam induced deposition *Appl. Phys. Lett.* **64** 1448
- [35] Kwitniewski S, Ptasinska-Denga E and Szmytkowski C 2003 Relationship between electron-scattering grand total and ionization total cross sections *Radiat. Phys. Chem.* **68** 169–74
- [36] Fowlkes J D, Randolph S J and Rack P D 2005 Growth and simulation of high-aspect ratio nanopillars by primary and secondary electron-induced deposition *J. Vac. Sci. Technol. B* **23** 2825–32